

Exploratory Combustion Synthesis: Amorphous Indium Yttrium Oxide for Thin-Film Transistors

Jonathan W. Hennek,^{†,§} Myung-Gil Kim,^{†,§} Mercouri G. Kanatzidis,^{*,†} Antonio Facchetti,^{*,†,‡} and Tobin J. Marks^{*,†}

[†]Department of Chemistry and the Materials Research Center, Northwestern University, 2145 North Sheridan Road, Evanston, Illinois 60208, United States

[‡]Polyera Corporation, 8045 Lamon Avenue, Skokie, Illinois 60077, United States

S Supporting Information

ABSTRACT: We report the implementation of amorphous indium yttrium oxide (a-IYO) as a thin-film transistor (TFT) semiconductor. Amorphous and polycrystalline IYO films were grown via a low-temperature solution process utilizing exothermic “combustion” precursors. Precursor transformation and the IYO films were analyzed by differential thermal analysis, thermogravimetric analysis, X-ray diffraction, atomic force microscopy, X-ray photoelectron spectroscopy, and optical transmission, which reveal efficient conversion to the metal oxide lattice and smooth, transparent films. a-IYO TFTs fabricated with a hybrid nanodielectric exhibit electron mobilities of $7.3 \text{ cm}^2 \text{ V}^{-1} \text{ s}^{-1}$ ($T_{\text{anneal}} = 300 \text{ }^\circ\text{C}$) and $5.0 \text{ cm}^2 \text{ V}^{-1} \text{ s}^{-1}$ ($T_{\text{anneal}} = 250 \text{ }^\circ\text{C}$) for 2 V operation.

The past decade has seen major advances in the field of materials for unconventional electronics.¹ Products such as smart windows, large-area active-matrix organic light-emitting diode (AMOLED) displays, printable radiofrequency identification (RF-ID) tags, and flexible displays all require the understanding-based implementation of new electronic materials.² To this end, crystalline and amorphous metal oxide semiconductors have been of great interest because of the possibility of coupling optical transparency and mechanical flexibility with excellent electrical performance. Indeed, the thin-film transistor (TFT) performance of many oxides exceeds that of amorphous silicon (a-Si:H), and their stability rivals or exceeds that of typical organic semiconductors.³ While metal oxide films have conventionally been grown by vapor-phase techniques such as atomic layer deposition, pulsed laser deposition,^{3b} chemical vapor deposition, and RF sputtering,⁴ solution-phase processes such as spin-coating,⁵ dip-coating,⁶ chemical bath deposition,⁷ inkjet printing,⁸ etc. offer the attraction of low-cost, high-throughput, roll-to-roll processing. Thus, excellent films of ZnO,⁹ In₂O₃,¹⁰ amorphous indium zinc oxide (a-IZO),¹¹ amorphous zinc indium tin oxide (a-ZITO),¹² and amorphous indium gallium zinc oxide (a-IGZO)¹³ can be grown from solution; however, the high required annealing/densification temperatures are typically incompatible with flexible polymer substrates.¹⁴

We recently reported a low-temperature route to mixed metal oxide films using a “combustion” process in which the heat required for oxide lattice formation is provided by the large

internal energies of the precursors (Figure 1A,B).¹⁵ In this method, an oxidizer and a fuel are combined in the precursor

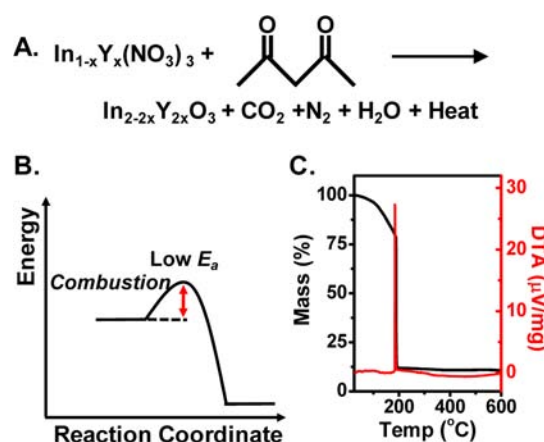


Figure 1. (A) Oxidizer + fuel pair scheme for the combustion synthesis of IYO. (B) Qualitative energetics of a combustion synthesis. (C) Thermal analysis of In_{1.95}Y_{0.05}O₃ film formation from a combustion precursor.

mixture, and mild annealing suffices to initiate an exothermic reaction within the film, affording smooth, flexible, and electrically active films. While In₂O₃, a-IZO, and amorphous zinc tin oxide (a-ZTO) films were demonstrated, the intriguing question arises as to whether this technique could be used for the exploratory synthesis of new oxide films, especially amorphous ones that might benefit from the low processing temperatures.

To achieve acceptable TFT performance (i.e., high mobilities and low carrier concentrations), small oxygen-binding cations such as Zn²⁺ or Ga³⁺ are typically introduced into In₂O₃ or SnO₂ hosts. Furthermore, mixing disparate metal ions promotes amorphous character and hence electrical uniformity, smooth surfaces, and flexibility due to the lack of grain boundaries. Recently, more strongly oxygen-binding group 3 and 4 cations, including Zr,¹⁶ Ti,¹⁷ Hf,¹⁸ and Sc,¹⁹ have been studied as matrix dopants to stabilize oxide lattices and suppress crystallization. Here we demonstrate a low-temperature route

Received: April 14, 2012

Published: May 24, 2012

to amorphous indium yttrium oxide (a-IYO) films having minimal Y doping, using combustion processing. A ternary system such as IYO is preferred to a quaternary system to reduce the number of potential electron scattering sites in the lattice. Also, incorporation of strongly oxygen-binding Y^{3+} can further reduce the number of charge scattering centers through amorphization at minimal doping levels. To date, Y doping of In_2O_3 has been reported only in bulk systems in high-temperature catalyst²⁰ or ferroelectric²¹ syntheses, and recent theoretical work suggests that Y incorporation into In_2O_3 should widen the band gap for greater transparency while preserving electron mobility.²² We report here that as little as 2.5 mol % Y doping effectively suppresses In_2O_3 crystallization at 250 °C, affording TFTs with high mobilities ($5.0 \text{ cm}^2 \text{ V}^{-1} \text{ s}^{-1}$) and low operating voltages (2 V) on a self-assembled nanodielectric. Furthermore, IYO provides optical transparency superior to that of In_2O_3 . Thin films of this novel semiconductor are very smooth when deposited by scalable spin-coating.

In and Y combustion precursor solutions were prepared from the nitrate salts at a total metal concentration of 0.05 M with acetylacetone + ammonia as the fuel. The Y molar concentration was varied from 2.5 to 25% in solutions aged for 13 h. Thin IYO films (~12 nm thick) were deposited by spin-coating the combined precursor solutions onto Si(100) substrates, annealing at 250 or 300 °C in air for 20 min, cooling to 25 °C, and then repeating this process three times. The thermal analysis data in Figure 1C reveal that ignition of the combustion precursors occurs at ~200 °C for the entire composition range. X-ray diffraction (XRD) data for the resulting IYO films annealed at 250 °C (Figure 2A) show that even for small Y concentrations, all of the films are amorphous. Thus, Y efficiently disrupts the In_2O_3 lattice, promoting the formation of amorphous materials. For 300 °C film annealing (Figure 2C), Y doping at ≤ 5 mol % yields polycrystalline films

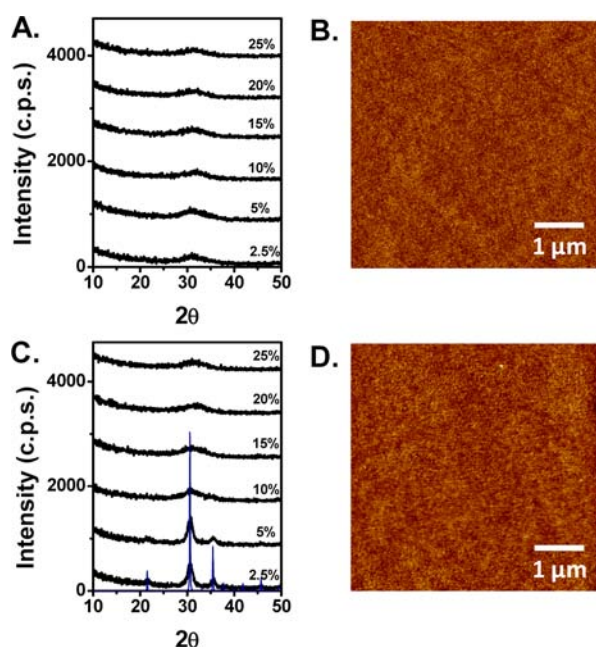


Figure 2. (A, C) XRD patterns for IYO films with varying Y content annealed at (A) 250 and (C) 300 °C. (B, D) AFM images of typical IYO films containing (B) 2.5 mol % Y at $T_{\text{anneal}} = 250$ °C and (D) 10 mol % Y at $T_{\text{anneal}} = 300$ °C.

with diffraction patterns matching that of In_2O_3 , while Y doping at ≥ 10 mol % significantly disrupts the In_2O_3 lattice, yielding amorphous films. Similar trends were observed in the XRD of IYO films annealed at elevated temperatures [Figure S1 in the Supporting Information (SI)]. Surface characterization by atomic force microscopy (AFM) reveals very smooth, featureless films with root-mean-square (rms) roughnesses in the 0.19–0.28 nm range (Figure 2B,D and Figures S2 and S3).

X-ray photoelectron spectroscopy (XPS) was used to analyze IYO surface impurities, carbon contamination, and oxygen binding (Figures S4 and S5). A survey scan reveals no organic impurities, in accord with previous combustion studies,¹⁵ and shows slow evolution of the Y 3p and 3d features at ~300 and 155 eV, respectively, as the amount of Y is increased. Detailed analysis of the carbon 1s spectrum reveals a slight increase in the peak centered at ~288.7 eV as the Y content is increased. This likely reflects the substantial basicity of Y_2O_3 , inducing reactions with CO_2 or other carbonaceous compounds in ambient air.²³ Evaluation of the O 1s features reveals that as the Y content is increased, a corresponding decrease in the 530.7 eV feature occurs, which is ascribable to the metal–oxygen–metal lattice.²⁴ Concurrently, surface or bulk M–OH species at 532.2 eV increase with increasing Y, in good agreement with the XRD analysis. All of the reported films exhibit excellent optical transparency (>90%) when deposited on glass (Figure S6).

TFTs were next fabricated on doped Si wafers with a thermally grown SiO_2 dielectric and Al source/drain electrodes deposited via thermal evaporation (channel length = 100 μm and width = 5 mm) to afford the final bottom-gate/top-contact structures $n^{++}\text{Si}/SiO_2(300 \text{ nm})/IYO/Al$. Experimental details and I – V plots are presented in the SI. Figure 3A,B shows typical transfer and output plots, and Figure 4A,B shows TFT performance metrics for $T_{\text{anneal}} = 250$ and 300 °C, respectively, for varied Y doping concentrations. At lower growth temperatures, a maximum mobility of $0.75 \text{ cm}^2 \text{ V}^{-1} \text{ s}^{-1}$ is achieved with a large current on/off ratio ($I_{\text{on}}/I_{\text{off}}$) of 10^5 – 10^6 and a threshold voltage (V_T) of 10 V. Notably, as the Y doping is increased, the mobility decreases significantly, and the devices become inactive at ≥ 20 mol % Y, which is not surprising since Y_2O_3 is a known high- κ dielectric.²⁶

Transistors annealed at 300 °C exhibit mobilities as high as $\sim 5 \text{ cm}^2 \text{ V}^{-1} \text{ s}^{-1}$ at ≤ 5 mol % Y. However, when the Y doping is increased to 10 mol %, the films became amorphous by XRD yet still maintain an excellent mobility of $2.2 \text{ cm}^2 \text{ V}^{-1} \text{ s}^{-1}$. This value is roughly twice those of a-Si:H and conventional solution-processed a-IGZO films annealed at 400 °C.²⁴ For both annealing temperatures, as the Y content is increased, the oxygen vacancy and free carrier concentrations decrease. As a result, $I_{\text{on}}/I_{\text{off}}$ initially increases because of the reduced I_{off} while a similar I_{on} is maintained. Further increases in Y content depress $I_{\text{on}}/I_{\text{off}}$ as a result of the significant decrease in I_{on} from the mobility degradation. On the other hand, V_T is related to the free carrier concentration and trap density. At low Y content, V_T follows the trend expected from the decrease in carrier concentration, further confirming the role of oxygen vacancy suppression. However, as the Y content is increased, we observe an unstable trend in V_T . We speculate that this result is related to reaction with the atmosphere, considering the basic nature of Y_2O_3 .²³ Investigations of device passivation and interface reactions are underway.

Next, a-IYO TFTs were fabricated on high- κ dielectric zirconia-based self-assembled nanodielectric (Zr-SAND) films

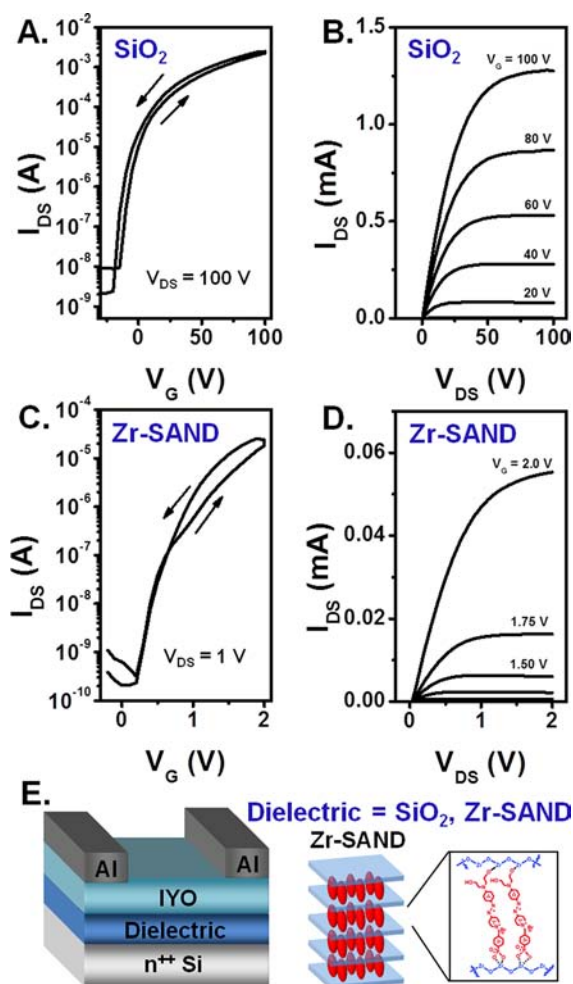


Figure 3. Typical (A, C) transfer and (B, D) output plots for a-IYO films with 2.5 mol % Y and $T_{\text{anneal}} = 250\text{ }^{\circ}\text{C}$ on (A, B) a SiO_2 gate dielectric and (C, D) a Zr-SAND gate dielectric. (E) Schematics of the TFT and Zr-SAND structures.²⁵

(Figure 3E)²⁵ having a thickness of $\sim 12\text{ nm}$ and a capacitance of 450 nF/cm^2 to demonstrate the compatibility of a-IYO with various dielectrics and low-voltage operation. Devices with the structure $n^{++}\text{Si}/\text{Zr-SAND}/\text{a-IYO}/\text{Al}$ were fabricated at $250\text{ }^{\circ}\text{C}/2.5\text{ mol \% Y}$ and at $300\text{ }^{\circ}\text{C}/10\text{ mol \% Y}$. Typical transfer and output plots (Figure 3C,D and Figure S9) exhibit saturation at low operating voltages and good pinch-off, with electron mobilities of 5.0 and $7.3\text{ cm}^2\text{ V}^{-1}\text{ s}^{-1}$ for 250 and $300\text{ }^{\circ}\text{C}$, respectively, at operating voltages of only 2.0 V (Table S1 in the SI). The superior performance of Zr-SAND/a-IYO TFTs versus $\text{SiO}_2/\text{a-IYO}$ TFTs is the result of the increased dielectric capacitance and decreased semiconductor–dielectric interface trap-state density.²⁷

These results demonstrate the first use of Y doping of In_2O_3 to generate amorphous semiconducting IYO films at low temperatures by combustion processing. The a-IYO TFTs exhibit excellent device performance when fabricated with Zr-SAND. This integration of combustion-derived amorphous oxide films with hybrid nanodielectrics points to future opportunities in novel materials design.

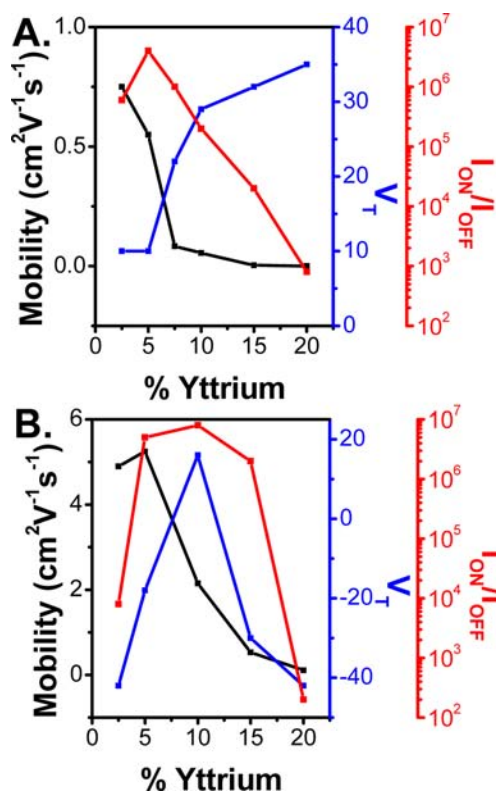


Figure 4. TFT data for IYO films having varied Y mol % annealed at (A) 250 and (B) $300\text{ }^{\circ}\text{C}$.

■ ASSOCIATED CONTENT

Supporting Information

Experimental details, XRD of IYO at high T_{anneal} , XPS spectra, additional AFM and rms roughness data, representative transfer and output plots for all of the fabricated TFTs, and performance metrics for Zr-SAND/a-IYO TFTs. This material is available free of charge via the Internet at <http://pubs.acs.org>.

■ AUTHOR INFORMATION

Corresponding Author

m-kanatzidis@northwestern.edu; a-facchetti@northwestern.edu; t-marks@northwestern.edu

Author Contributions

[§]J.W.H. and M.-G.K. contributed equally.

Notes

The authors declare no competing financial interest.

■ ACKNOWLEDGMENTS

We thank ONR (MURI N00014-11-1-0690), AFOSR (FA9550-08-1-0331), the Northwestern Materials Research Science and Engineering Center (NSF DMR-1121262), and Polyera Corp. for support of this research. Microscopy studies were performed in the NIFTI and KECK II facilities of the NUANCE Center at Northwestern University, which is supported by NSF-NSEC, NSF-MRSEC, the Keck Foundation, the State of Illinois, and Northwestern University.

■ REFERENCES

- (1) Jeong, S.; Moon, J. *J. Mater. Chem.* **2012**, *22*, 1243–1250.
- (2) Zhang, L.; Di, C.-a.; Yu, G.; Liu, Y. *J. Mater. Chem.* **2010**, *20*, 7059–7073.
- (3) Mizoguchi, H.; Kamiya, T.; Matsuishi, S.; Hosono, H.

Nat. Commun. **2011**, *2*, 470. (d) Wu, J.; Agrawal, M.; Becerril, H. A.; Bao, Z.; Liu, Z.; Chen, Y.; Peumans, P. *ACS Nano* **2010**, *4*, 43–48.

(2) (a) Sun, Y. G.; Rogers, J. A. *Adv. Mater.* **2007**, *19*, 1897–1916. (b) Ortiz, R. P.; Facchetti, A.; Marks, T. J. *Chem. Rev.* **2010**, *110*, 205–239. (c) Arias, A. C.; MacKenzie, J. D.; McCulloch, I.; Rivnay, J.; Salleo, A. *Chem. Rev.* **2010**, *110*, 3–24. (d) Hu, X.; Krull, P.; de Graff, B.; Dowling, K.; Rogers, J. A.; Arora, W. J. *Adv. Mater.* **2011**, *23*, 2933–2936.

(3) (a) Wager, J. F. *Science* **2003**, *300*, 1245–1246. (b) Nomura, K.; Ohta, H.; Takagi, A.; Kamiya, T.; Hirano, M.; Hosono, H. *Nature* **2004**, *432*, 488–492. (c) Ju, S. Y.; Facchetti, A.; Xuan, Y.; Liu, J.; Ishikawa, F.; Ye, P. D.; Zhou, C. W.; Marks, T. J.; Janes, D. B. *Nat. Nanotechnol.* **2007**, *2*, 378–384. (d) *Transparent Electronics*; Marks, T. J., Facchetti, A., Eds.; Wiley-VCH: West Sussex, U.K., 2010.

(4) Yabuta, H.; Sano, M.; Abe, K.; Aiba, T.; Den, T.; Kumomi, H.; Nomura, K.; Kamiya, T.; Hosono, H. *Appl. Phys. Lett.* **2006**, *89*, No. 112123.

(5) Kim, H. S.; Kim, M.-G.; Ha, Y.-G.; Kanatzidis, M. G.; Marks, T. J.; Facchetti, A. *J. Am. Chem. Soc.* **2009**, *131*, 10826–10827.

(6) Lee, H.; Dellatore, S. M.; Miller, W. M.; Messersmith, P. B. *Science* **2007**, *318*, 426–430.

(7) Cheng, H.-C.; Chen, C.-F.; Lee, C.-C. *Thin Solid Films* **2006**, *498*, 142–145.

(8) Lee, D. H.; Chang, Y. J.; Herman, G. S.; Chang, C. H. *Adv. Mater.* **2007**, *19*, 843–847.

(9) (a) Bong, H.; Lee, W. H.; Lee, D. Y.; Kim, B. J.; Cho, J. H.; Cho, K. *Appl. Phys. Lett.* **2010**, *96*, No. 192115. (b) Hoffmann, R. C.; Dilfer, S.; Issanin, A.; Schneider, J. J. *Phys. Status Solidi A* **2010**, *207*, 1590–1595.

(10) Wang, L.; Yoon, M.-H.; Facchetti, A.; Marks, T. J. *Adv. Mater.* **2007**, *19*, 3252–3256.

(11) Choi, C. G.; Seo, S.-J.; Bae, B.-S. *Electrochem. Solid-State Lett.* **2008**, *11*, H7–H9.

(12) Kim, M.-G.; Kim, H. S.; Ha, Y.-G.; He, J.; Kanatzidis, M. G.; Facchetti, A.; Marks, T. J. *J. Am. Chem. Soc.* **2010**, *132*, 10352–10364.

(13) Kamiya, T.; Nomura, K.; Hosono, H. *Sci. Technol. Adv. Mater.* **2010**, *11*, No. 044305.

(14) Banger, K. K.; Yamashita, Y.; Mori, K.; Peterson, R. L.; Leedham, T.; Rickard, J.; Sirringhaus, H. *Nat. Mater.* **2011**, *10*, 45–50.

(15) Kim, M.-G.; Kanatzidis, M. G.; Facchetti, A.; Marks, T. J. *Nat. Mater.* **2011**, *10*, 382–388.

(16) Tsay, C.-Y.; Fan, K.-S. *Mater. Trans.* **2008**, *49*, 1900–1904.

(17) Chong, H. Y.; Han, K. W.; No, Y. S.; Kim, T. W. *Appl. Phys. Lett.* **2011**, *99*, No. 161908.

(18) Kim, C.-J.; Kim, S.; Lee, J.-H.; Park, J.-S.; Kim, S.; Park, J.; Lee, E.; Lee, J.; Park, Y.; Kim, J. H.; Shin, S. T.; Chung, U.-I. *Appl. Phys. Lett.* **2009**, *95*, No. 252103.

(19) Choi, Y.; Kim, G. H.; Jeong, W. H.; Bae, J. H.; Kim, H. J.; Hong, J.-M.; Yu, J.-W. *Appl. Phys. Lett.* **2010**, *97*, No. 162102.

(20) Qin, Z.; Liang, Y.; Liu, Z.; Jiang, W. J. *Environ. Sci.* **2011**, *23*, 1219–1224.

(21) (a) Dixit, A.; Smith, A. E.; Subramanian, M. A.; Lawes, G. *Solid State Commun.* **2010**, *150*, 746–750. (b) Jiang, P.; Li, J.; Sleight, A. W.; Subramanian, M. A. *Inorg. Chem.* **2011**, *50*, 5858–5860.

(22) (a) Aliabad, H. A. R.; Hosseini, S. M.; Kompany, A.; Youssefi, A.; Kakhki, E. A. *Phys. Status Solidi B* **2009**, *246*, 1072–1081. (b) Kompany, A.; Aliabad, H. A. R.; Hosseini, S. M.; Baedi, J. *Phys. Status Solidi B* **2007**, *244*, 619–628. (c) Hosseini, S. M.; Aliabad, H. A. R.; Kompany, A. *Mod. Phys. Lett. B* **2010**, *24*, 2251–2265.

(23) Kwo, J.; Hong, M.; Kortan, A. R.; Queeney, K. L.; Chabal, Y. J.; Opila, R. L.; Muller, D. A.; Chu, S. N. G.; Sapjeta, B. J.; Lay, T. S.; Mannaerts, J. P.; Boone, T.; Krautter, H. W.; Krajewski, J. J.; Sergnt, A. M.; Rosamilia, J. M. *J. Appl. Phys.* **2001**, *89*, 3920–3927.

(24) Jeong, S.; Ha, Y. G.; Moon, J.; Facchetti, A.; Marks, T. J. *Adv. Mater.* **2010**, *22*, 1346–1350.

(25) Ha, Y. G.; Emery, J. D.; Bedzyk, M. J.; Usta, H.; Facchetti, A.; Marks, T. J. *J. Am. Chem. Soc.* **2011**, *133*, 10239–10250.

(26) (a) Adamopoulos, G.; Thomas, S.; Bradley, D. D. C.; McLachlan, M. A.; Anthopoulos, T. D. *Appl. Phys. Lett.* **2011**, *98*,

No. 123503. (b) Rastogi, A. C.; Sharma, R. N. *J. Appl. Phys.* **1992**, *71*, 5041–5052. (c) Lin, C.-M.; Shih, W.-c.; Chang, I. Y.-k.; Juan, P.-C.; Lee, J. Y.-m. *Appl. Phys. Lett.* **2009**, *94*, No. 142905.

(27) (a) Wang, L.; Yoon, M. H.; Lu, G.; Yang, Y.; Facchetti, A.; Marks, T. J. *Nat. Mater.* **2006**, *5*, 893–900. (b) Kangho, L.; Gang, L.; Facchetti, A.; Janes, D. B.; Marks, T. J. *Appl. Phys. Lett.* **2008**, *92*, No. 123509. (c) Ju, S.; Ishikawa, F.; Chen, P.; Chang, H.-K.; Zhou, C.; Ha, Y.-g.; Liu, J.; Facchetti, A.; Marks, T. J.; Janes, D. B. *Appl. Phys. Lett.* **2008**, *92*, No. 222105.